

Palbociclib CDK4/6- and Crizotinib MET/ALK/ROS1-inhibitors Synergize to Enhance Senescence and Immune Recognition in Melanoma Cells Independently of *BRAF/NRAS* Status

Fan Zhang^{1*}, Lola Boutin^{1*}, Ishani Das^{2*}, Jeroen Melief^{2*}, Madhurendra Singh^{1*}, Marina Stantic^{1*}, Mohammad Alzrigat^{1**}, Alireza Azimi^{2**}, Lucas Baldran^{2**}, Wesam Bazzar^{3**}, Michelle Da Silva Liberio^{1**}, Jacob Goodwin^{1**}, Rainer Tuominen^{2**}, Veronica Höiom^{2**}, Fredrik Jerhammar^{2**}, Suzanne Egyhazi Brage^{2#}, Johan Hansson^{2#}, Rolf Kiessling^{4#}, Galina Selivanova^{1#}, Klas G. Wiman^{2#}, Margareta Wilhelm^{1#}, and Lars-Gunnar Larsson^{1,3#&}.

¹Department of Microbiology, Tumor and Cell Biology and ²Department of Oncology-Pathology, Karolinska Institutet, Stockholm, Sweden, ³Department of Pharmaceutical Biosciences, Uppsala University, Sweden, ⁴Theme Cancer, Patient area Head and Neck, Lung and Skin Cancer, Karolinska University Hospital, Stockholm, Sweden.

Running title: Palbociclib and Crizotinib Synergize to Target Melanoma Cells

*These authors contributed equally to the publication.

**These authors contributed equally to the publication.

#Equally contributing senior authors.

&Corresponding author: Lars-Gunnar Larsson, Department of Pharmaceutical Biosciences, Uppsala University, Biomedical Center (BMC), Husargatan 3, 75124 Uppsala, Sweden.

E-mail: Lars-Gunnar.Larsson@uu.se.

Conflict of interest statement

LGL is cofounder of MyCural Therapeutics AB and has ownership interests in this company.

KGW is cofounder and shareholder of Aprea Therapeutics, a company that develops novel anticancer therapy including APR-246 (Eprenetapopt). KGW has previously obtained research funding and salary from Aprea Therapeutics. KGW is board member of MyCural Therapeutics AB. LBo is founder of T-Hope Nordics AB and has ownership interests in this company.

Abstract

“Pro-senescence therapy”, which triggers both permanent cell cycle arrest and an immune response, is a controversial new strategy for cancer treatment. To assess this strategy in melanoma, we performed a high throughput microscopy-based senescence screen utilizing a panel of melanoma cell lines with different driver mutations and a collection of clinical and experimental drugs. We found that vemurafenib and trametinib, which inhibit BRAF^{V600E} and MEK1/2, respectively, induced senescence in some but not all BRAF-mutant cell lines. In contrast, palbociclib, BKM-120 and crizotinib, which inhibit CDK4/6, PI3K, and MET/ALK/ROS1, respectively, triggered senescence in most cell lines, irrespective of BRAF/NRAS mutation status, and overcame intrinsic and acquired vemurafenib resistance. The combination of palbociclib and crizotinib synergized to further enhance the senescence response in all cell lines irrespective of BRAF/NRAS mutation status, increased the expression of SASP factors, such as IL-1 α and β , and HLA class I and other markers for recognition by NK and T cells. Further, this combination caused a significant increase in CD8⁺ T cells and pro-inflammatory macrophages in the tumor microenvironment and a marked reduction of mouse melanoma tumor growth that was dependent on CD8⁺ T cells, suggesting increased immune surveillance. Our findings suggest that pro-senescence therapy based on concomitant inhibition of both CDK4/6 and MET/ALK/ROS1 could be developed further as an alternative treatment strategy for melanoma.

Significance: Pro-senescence therapy based on combined targeting of CDK4/6 with Palbociclib and MET/ALK/ROS1 with Crizotinib inhibits melanoma tumor growth through anti-tumor immune response activation, providing an alternative treatment strategy for malignant melanoma.

Introduction

The incidence of cutaneous malignant melanoma is increasing at one of the fastest rates among all cancer types, and it remains the skin cancer with highest mortality rate, causing around 55 000 deaths per year worldwide (1). Approximately 50% of advanced cutaneous melanomas carry a *BRAF* mutation, most commonly *BRAF*^{V600E}, while about 25% harbor mutations in *NRAS* (2,3); both genes are upstream regulators of the MAP kinase pathway. The development of specific inhibitors targeting the mutated *BRAF*^{V600E} kinase and selective inhibitors of the downstream MEK1/2 kinases have drastically improved treatment outcome of advanced melanoma for more than a decade (4-6). A key feature of melanoma is its very high load of somatic mutations (2) resulting in neoantigens that can be recognized by the immune system. Consequently, the introduction of immune checkpoint inhibitors (ICI) blocking PD-1, CTLA-4 or other checkpoint molecules which stimulate T-cell engagement in the anti-tumor immune response was a major breakthrough. This has significantly improved survival in patients with advanced melanoma over the past 15 years (7,8). However, *BRAF*/*MEK* therapies are only effective in 50% of cases with the *BRAF*^{V600E}-mutation, and immunotherapies have also provided beneficial effects in around 50% of the cases (1). In addition, most metastatic cancers eventually develop resistance to targeted therapies, leaving a large portion of advanced melanoma with limited treatment options (1,9), emphasizing the urgent need for new therapeutic strategies.

During the last decade, the concept of “therapy-induced senescence” (TIS) or “pro-senescence therapy” has emerged as an alternative strategy to combat cancer (10-12). Cellular senescence - defined as permanent cell cycle arrest - is along with apoptosis a main barrier against tumor development (13). It also plays an important role during embryogenesis and in adults during tissue repair and renewal (14). Senescence is triggered by different types of stress, e.g. aberrant oncogene expression (oncogene-induced senescence (OIS)), telomere dysfunction, oxidative and endoplasmic reticulum (ER) stress and DNA damage caused by for instance chemotherapeutic drugs or irradiation (10,12,15,16). As an example of OIS,

oncogenic BRAF is a potent inducer of senescence in premalignant melanocytes in nevi of the skin, while progression to malignant melanoma is accompanied by evasion of senescence (17,18). The senescence process is usually driven by two major tumor suppressor pathways, i.e. p53/p21 and p16/pRB pathways (10,12,19). However, there is a variety of senescence phenotypes described, depending on the senescence trigger, cell type and microenvironment (20-22). An important aspect of the senescent phenotype is the senescence-associated secretory phenotype (SASP) (23,24). The biological function of SASP is to maintain the senescent state and to induce innate and adaptive immune responses leading to clearance of senescent cells, including senescent tumor cells (10,12,19,21,25,26). On the other hand, there is also multiple evidence suggesting that SASP components can promote tumor progression by stimulating inflammation, epithelial to mesenchymal transition (EMT), stemness, immune suppression, and other tumor-promoting processes, thereby undermining senescence-induced tumor suppression (10,12,21,25,27,28). In addition, tumor cells can escape senescence due to for instance loss/inactivation of *TP53*, *CDKN2A* (encoding p16 and p19ARF), *PTEN* or other tumor suppressors (3), or by activation of *MYC* (18,29,30).

Senescence and SASP can therefore be viewed as a double-edged sword in cancer development and progression. To overcome the negative sides of senescence, many efforts during recent years have attempted to introduce senolytics, i.e. substances that kill senescent cells, and senomorphics, i.e. substances that promote the “good” and prevent the “bad” sides of senescence, in order to promote immune surveillance of senescent cells and/or prevent senescence escape of tumor cells (10,12,31).

To explore the potential role of pro-senescence therapy in melanoma treatment, we performed a drug screen on a panel of melanoma cell lines representing the most common driver mutations and copy number alterations in human melanoma, including *BRAF*^{V600E}, *NRAS*^{Q61R}, *CDKN2A*, *PTEN*, *TP53*, *CDK4*, and *CCND1*. We show here that several of the drugs tested, either alone or in combination, particularly palbociclib combined with crizotinib, induce senescence and upregulate immune markers known to promote immune clearance in a broad range of melanoma cells. Further, combined treatment with palbociclib and crizotinib

reduced tumor growth and stimulated infiltration of CD8+ T cells and M1-type macrophages in an immunocompetent melanoma mouse model.

Materials & Methods

Cell culture

The human melanoma cell lines used are listed in Table 1. A375, SKMEL2, SKMEL28 and YUMM1.7 cells were purchased from the American Type Culture Collection (ATCC). The ESTDAB cell lines were obtained from European searchable Tumor cell Bank and database (ESTDAB), Germany (<http://www.ebi.ac.uk/ipd/estdab>). The early-passage KADA melanoma cell line was established from a stage III melanoma patient undergoing treatment in the oncology clinic at Karolinska University Hospital (32). A375-VR4 is a vemurafenib-resistant subline derived from A375 cells (33). Media for different melanoma cell lines are indicated Supplementary Table 1B, supplemented with 10% fetal bovine serum (FBS) (Gibco), 2 mM L-glutamine, 50 U/ml of penicillin and 50 mg/ml of streptomycin (ThermoScientific). The YUMM1.7 mouse melanoma cell line (34) was cultured in DMEM: F12 GlutaMAX™ supplement (Thermo Fisher), supplemented with 10% FBS, 1% penicillin and streptomycin, and 1X MEM Non-Essential Amino Acids (Thermo Fisher). Cells were maintained in an incubator at 37 °C with 5% CO₂ and optimal humidity. All cell lines used were negative for mycoplasma.

Drugs and compounds

The drugs and compounds, the concentrations used, and their sources are listed in Table 1, Supplemental Table 1A and Supplemental Table 2.

Whole genome sequencing

DNA was extracted from all cell lines used using Allprep universal kit. This DNA was quantified using NanoDrop 2000 instrument and 100 ng was subjected to whole genome sequencing (WGS) using library build-up with the Nextera DNA library prep, Illumina platform and in-house developed post-read filtering (Science for Life Laboratory, Stockholm, Sweden). The resulting reads were mapped and variants called, filtering for variants in the coding regions

and excluding indels, using the Partek Flow lab edition software and DNA-Seq Toolkit for Partek Flow.

High-throughput drug screen for mono-therapy

Cells were seeded at the cell densities indicated in Supplementary Table 1B in 384-well plates upon different drug treatment for 72 hours on black clear bottom imaging quality 384-well plates (Corning, cat # 3985). Prior to fixation, cells were incubated with 5 μ M EdU reagent (Thermo Scientific) for 30 min. Then cells were fixed with 4% PFA, permeabilized with 0.3% Triton-X100, blocked with 2% BSA. EdU detection was performed first according to the manufacturer's protocol. For other biomarkers, cells were incubated with phalloidin (Thermo Scientific) or different primary antibodies (see Supplementary Materials and Methods) at 4 $^{\circ}$ C overnight before counterstaining with DAPI (Thermo Scientific). Imaging was performed with Olympus scan^R high-content imager with a 10x objective. Intensities per field were collected and after normalizing to DMSO, median values (%) were displayed in heatmaps, which was generated via Morpheus (<https://software.broadinstitute.org/morpheus>).

Drugs were dissolved in DMSO at indicated stock concentration in Suppl. Table 1A, and stored in -20 $^{\circ}$ C.

Cell cycle analysis

Cell cycle analysis was performed as described in (35) using 5-Ethynyl-2'-Deoxyuridine (EdU) Staining and Flow Cytometry. In brief, prior to harvesting, the cells were pulsed with 10 μ M EdU for 90 min, harvested, stained according to manufacturer's instructions, and analyzed by FACSCalibur (BD Biosciences). Cell cycle analysis was performed by FlowJo software.

Senescence-associated β -galactosidase activity (SA- β -gal) assays

Drug induced senescence was investigated by assessing β -galactosidase activity using the quantitative SA- β -gal MUG assay (36) or by x-gal senescence-associated β -galactosidase staining, pH 6 (#9860 staining kit, Cell Signaling Technology), as described in detail (37) (see also Supplementary Materials and Methods). Cells were treated with indicated drugs for 3-5 days before harvesting. All MUG assay reagents were purchased from Sigma-Aldrich. The amount of fluorescent product was measured using a Tecan microplate reader (Tecan Trading AG). X-gal SA- β -gal staining was assessed by light microscopy.

RNA and protein extraction, real-time PCR and western blot analysis

Total RNA was extracted using the Aurum™ Total RNA Mini Kit (Bio-Rad) following the standard manufacturer's protocol. For relative quantification of mRNAs, one µg total RNA was reverse transcribed to cDNA using the iScript™ cDNA Synthesis Kit (Bio-Rad) according to the manufacturer's instructions. Real-time PCR was conducted with SsoAdvanced™ Universal SYBR® Green Supermix in 384 well format using CFX384 real-time system (Bio-Rad). For primer sequences, see Supplementary Materials and Methods. The relative expression of genes was determined using the Bio-Rad CFX Maestro software. The data were presented as $2(-\Delta\Delta CT)$.

Protein extraction was performed using RIPA buffer (25 mM Tris-HCl pH 7.6, 150 mM NaCl, 1% NP-40, 1% sodium deoxycholate, 0.1% SDS), 1 mM NaOV, protease and phosphatase inhibitors as described (38). Protein concentration was measured using BCA kit according to manufacturer's protocol (Thermo Scientific).

40-50 µg of protein was loaded on a 4-12% NuPage Bis-Tris gel (Thermo Scientific), transferred onto a 0.45 µm PVDF membrane (Millipore), blocked using 5% BSA/milk and incubated with the primary overnight at 4°C. Following day, the membranes were washed with 1X TBST (3X, 10 min wash each) and incubated with the appropriate HRP-labeled secondary antibodies (Cell signaling Technology) for 1h, followed by ECL based detection using Image Quant LAS 4000 (GE Healthcare Europe GmbH, Freiburg, Germany). Primary antibodies used are listed in Supplementary Materials and Methods.

High-throughput drug screen for combination-therapy

Approximately 3000-5000 cells were seeded in 96-well plates and treated with a variety of drug combinations for 72 hours. Cells were fixed with 4% paraformaldehyde (Sigma), permeabilized with 0.5% Triton X-100 (Sigma), blocked with 4% BSA (Sigma), and then stained with phalloidin (Thermo Scientific) and counterstained with DAPI. Cell number, nuclear/cell size and EdU incorporation were examined by automated fluorescent imaging system ImageXpress Micro (Molecular Devices). Image analysis were done via CellProfiler and mean values were presented as heatmaps via Morpheus (<https://software.broadinstitute.org/morpheus>). Combenefit software was used to calculate combination index (39), where HSA model was applied for synergism/antagonism definition and displayed as heatmaps via online Morpheus software (<https://software.broadinstitute.org/morpheus/>).

Flow cytometry

Flow cytometry was performed using a Novocyte 2000 flow cytometer (Acea Biosciences, San Diego, CA, USA). Primary antibodies used are listed in Supplementary Materials and Methods. LIVE/DEAD Fixable Aqua Dead Cell Stain (Thermo Scientific) was included as a viability dye in all experiments to enable exclusion of non-viable cells in our analyses. Analysis was done using FlowJo software version 10 (Treestar). The results are expressed as geomean fluorescence intensity (geoMFI) of at least three independent experiments.

Melanoma mouse model

All animal experiments were performed in accordance with the guidelines of the Karolinska Institutet and approved by the Stockholm North Ethics Committee for Animal Research (ethical approval 10025/23). Five- to six-week-old female C57BL/6J mice were subcutaneously injected with 2.5×10^5 YUMM1.7 cells mixed in 100uL PBS/Geltrex (75:25). Tumor size was measured and recorded three times per week using the formula $V = (L \times W^2)/2$. Drug treatment began when the tumors were palpable. Animals were divided into treatment groups and treated with 180uL oral gavage according to these groups: Group 1: vehicle (0.5% methylcellulose, 0.5% Tween80), Group 2: 80mg/kg palbociclib diluted in vehicle, Group 3: 60mg/kg crizotinib diluted in vehicle, Group 4: 80mg/kg palbociclib + 60mg/kg crizotinib diluted in vehicle. At the end of treatment, tumors were harvested, weighed, and subjected to flow cytometric analysis. To deplete CD8+ T cells, 200ug/mouse InVivoMab anti-mouse CD8a clone 2.43 (Bioxcell, BR0061) or InVivoMab rat IgG2b isotype control (Bioxcell, BE0090) were diluted in InVivoPure pH7 dilution buffer (Bioxcell, IP0070), and injected i.p. two days before the start of drug treatment, followed by administration of 100ug/mouse every 4 days during the course of tumor growth. The depletion efficiency was above 98 % as determined by flow cytometry.

Immune infiltration in YUMM1.7 tumors

Harvested tumors were cut into small pieces in RPMI 1640 media serum free using razor blades. Enzymatic and mechanical dissociation was performed using the mouse tumor dissociation kit (130-096-730, Milteniy) and the gentleMACS™ Dissociator (130-093-235, Milteniy) according to the manufacturer's specifications. Cell debris was removed by

centrifugation 100xg for 10 minutes. Red blood cells were removed using RBC lysis buffer (MIK1512, Karolinska Hospital) for 5 minutes at room temperature. FcγR was blocked before staining using Fc Block anti mouse CD16/CD32 (clone 93, Biolegend) for 5 minutes at 4°C. The primary antibodies used for flow cytometry are listed in Supplementary Materials and Methods. All data were acquired on a BD LSRII or Fortessa flow cytometer (BD Bioscience). Analysis was done using FlowJo software version 10 (Treestar). The quality control of the raw data was performed using the flowAI plugin in FlowJo and only the “GoodEvents” population was kept for further analysis (40).

Statistical analysis

One-way ANOVA with post-hoc Dunnett’s multiple comparison test was applied used and performed via GraphPad Prism version 10.00 (for Windows, GraphPad Software, La Jolla California USA, www.graphpad.com), at a level of significance $\alpha=0.05$.

Data Availability

The data generated in this study are available upon request from the corresponding author.

Results

Drug therapy-induced senescence screening in melanoma cell lines

To identify drugs with senescence-inducing activity in melanoma, a senescence screen was set up using a panel of eleven human melanoma cell lines (Fig. 1A and Table 1), representing some of the most common driver mutations in melanoma. A set of conventional and targeted drugs and compounds of relevance for melanoma and pro-senescence therapy, either already in clinical use or at an experimental stage were selected, including vemurafenib (4), trametinib (5), BKM120 (41), palbociclib (42), crizotinib (43), and seliciclib (44), inhibiting BRAF^{V600E}, MEK1/2, PI3K, CDK4/6, ALK/MET/ROS1, CDK2/7/9, respectively, and the DNA alkylating agent temozolomide (45). In addition, the p53-activating molecules Nutlin-3A (46), RITA (47) and APR-246 (Eprenetapopt) (48) were included (Table 1). The screening was performed using a high-throughput multicolor immunofluorescence microscopy system (Fig. 1A, Suppl. Tables 1

and 2), staining for DAPI (cell number), phalloidin (cell size), EdU incorporation (replication), H3K9me3 (senescence-associated heterochromatin foci) and p53, thereby covering many essential markers of senescence suitable for fluorescence staining (15) as well as HLA class I (antigen recognition by T cells). The criterion for a major senescence response was the combination of reduced cell number and EdU incorporation, increased cell size, elevated H3K9me3 and p53 expression. While cell cycle arrest is an obligatory criterion, increased expression of only one or some other markers would be considered “partial senescence” or a “senescence-like” phenotype.

The results of the screen are presented as heatmaps in Fig. 1B-D (five selected representative cell lines) and Suppl. Fig. S1A-C (all 11 cell lines). Inhibition of BRAF^{V600E} with vemurafenib induced a major senescence response in two of the BRAF^{V600E}-mutant cell lines, A375 and ESTDAB-049, but not in SKMEL28 and ESTDAB37 (Fig. 1B and Suppl. Fig. S1A), indicating that the latter possess an intrinsic resistance to BRAF^{V600E} inhibition, possibly due to additional driver mutations and/or copy number alterations (Table 1). We observed a clear senescence response to the MEK1-inhibitor trametinib in all BRAF^{V600E}-mutant cell lines, but poor response in two out of three cell lines with NRAS mutation and in the non-BRAF/NRAS mutant cell lines, (Fig. 1C and Suppl. Fig. S2B, C). Most cell lines were essentially non-responsive to temozolomide at the concentrations used.

Interestingly, palbociclib, BKM120 and crizotinib efficiently induced senescence in all or most cell lines irrespective of BRAF/NRAS mutation status. Likewise, the CDK2 inhibitor seliciclib induced senescence in many of the cell lines of all categories. The p53:MDM2 interaction inhibitors Nutlin-3A and RITA induced senescence responses to a greater extent in wt TP53 cell lines and less in cell lines with mutant TP53 (Table 1) and vice versa for APR-246, which targets mutant p53 and disrupts redox homeostasis (49).

Palbociclib, BKM120 and crizotinib induce senescence and HLA class I expression in melanoma cells irrespective of BRAF/NRAS mutation status

The results from the senescence screen suggested that palbociclib, BKM120 and crizotinib induced either prominent or partial senescence in all eleven melanoma cell lines regardless

of *BRAF/NRAS* mutation status, including *BRAF*-mutant cells resistant to vemurafenib and trametinib. The responses to these drugs were further validated in five selected representative cell lines; vemurafenib sensitive/resistant *BRAF*^{V600E} mutant (A375, ESTDAB37), *NRAS*^{Q61R} mutation (SKMEL2), non-*BRAF/NRAS*-mutant (ESTDAB140, KADA) using an expanded set of senescence markers, including in addition to those used above also cell cycle distribution and additional molecular markers.

The results confirmed that vemurafenib induced senescence in a dose-dependent manner in A375 cells, as evidenced by an increase in cell/nuclear size and H3K9me3 staining intensity along with reduced EdU incorporation, decreased phosphorylation (i.e. activation) of pRb and cyclin B1 expression and an accumulation of cells in the G1 or G2 phases of the cell cycle (Fig. 2A-C, Suppl. Fig. S2). In contrast, vemurafenib failed to induce most markers of senescence in the *BRAF*^{V600E}-mutant ESTDAB37 cells and in the non-*BRAF*-mutant cell lines. Trametinib induced a good senescence response in *BRAF/NRAS*-mutant but a weak response in the non-*BRAF/NRAS*-mutant cells (Fig. 2A-C, Suppl. Fig. S2). Treatment with the CDK4/6 inhibitor palbociclib significantly increased cell/nuclear size and H3K9me3, decreased EdU incorporation, pRb phosphorylation and cyclin B expression, and caused G1 arrest, indicative of major senescence response in all five lines, but did not affect cell size in ESTDAB140 cells (Fig. 2A-C, Suppl. Fig. S2). The PI3 kinase inhibitor BKM120 and the ALK/MET/ROS1 inhibitor crizotinib induced significant changes for most senescence markers in all the cell lines, although with some differences between cell lines and senescence markers (Fig. 2A-C, Suppl. Fig. S2). There were no signs of apoptosis induction by any of the drugs at concentrations used, as determined by cleaved caspase 3 expression, except for trametinib in SKMEL2 cells (Suppl. Fig 2E).

We also validated whether senescence-inducing drugs affected the expression of HLA class I (Fig 1, Suppl. Fig. 1, Fig 2 D). Vemurafenib increased HLA class I expression in A375 cells, but not in ESTDAB37 cells or any of the other cell lines. Trametinib increased HLA class I expression in the *BRAF* or *NRAS*-mutant cell lines and slightly in KADA cells. Remarkably, palbociclib, BKM120 and crizotinib strongly induced expression of HLA class I in all the cell lines.

In summary, while vemurafenib and trametinib induced senescence and HLA class I expression in a subset of cell lines related to *BRAF/NRAS* mutation status, palbociclib, BKM120 and

crizotinib treatments resulted in a pronounced senescence response and HLA class I expression in all cell lines regardless of *BRAF/NRAS* mutation status.

Palbociclib, crizotinib and BKM120 synergize with vemurafenib to induce senescence in vemurafenib-resistant *BRAF*^{V600E}-mutant melanoma cell lines

The results of the mono-treatments showed that palbociclib, BKM120 and crizotinib induced senescence in all four *BRAF*^{V600E}-mutant cell lines, including ESTDAB37 cells that were resistant to vemurafenib-induced senescence. We were therefore interested in whether these drugs would synergize with vemurafenib to overcome vemurafenib resistance. We selected A375 as a control for vemurafenib-sensitive cells, while A375-VR4 (a vemurafenib-resistant subline derived from A375) (33) and ESTDAB37 served as two vemurafenib-resistant cell lines with *BRAF*^{V600E} mutation.

As shown in the heatmaps in Fig. 3, the combination of vemurafenib and palbociclib efficiently reduced cell number and induced cell cycle arrest and cell enlargement, i.e. signs of senescence induction in A375, A375-VR4 and ESTDAB37 cells. Calculation of the synergy between the two drugs based on the data of cell size using combination index showed a strong synergistic effect as visualized in the heat maps to the far right on each panel (Fig. 3A-C). The synergism was particularly strong in the vemurafenib-resistant lines A375-VR4 and ESTDAB37. The combination of vemurafenib with temozolomide, BKM120, crizotinib or trametinib had some synergistic effects in all three cell lines, but less than the combination vemurafenib + palbociclib (Fig. 3, Suppl. Fig. S3).

We also investigated combination treatments with the MEK1/2 inhibitor trametinib together with palbociclib, BKM120, crizotinib, temozolomide, APR-246 or RITA in the non-*BRAF/NRAS* mutant cell line KADA, which has a truncating mutation in *NF1* – a regulator of the RAS pathway. Suppl. Fig. S4 shows that all these drugs and compounds synergized with trametinib to some extent.

Palbociclib and crizotinib synergistically enhance senescence in melanoma cells irrespective of *BRAF/NRAS* mutation status

Since palbociclib, BKM120 and crizotinib induced prominent or partial senescence in all melanoma cell lines irrespective of *BRAF/NRAS* mutation status (Fig. 1, 2 and Suppl. Fig. S1, S2), we next addressed the question whether these three drugs might work cooperatively. Therefore, we performed a screen with the same layout as above with the combination palbociclib+BKM120, palbociclib + crizotinib and BKM120 + crizotinib on A375, A375-VR4, ESTDAB 37, KADA and ESTDAB140 cells. While the combinations palbociclib+BKM120 and BKM120+crizotinib produced rather weak synergizes except for palbociclib + BKM120 in KADA cells (Fig. 4A, Suppl. Fig. S5 and Suppl. Fig. S6), the combination palbociclib plus crizotinib showed strong synergistic effects on senescence induction in all five melanoma cell lines (Fig. 4A and Suppl. Fig. S5). Considering also the limited clinical activity and tolerability of BKM120 in recent clinical trials (50), we therefore decided to focus on the combination palbociclib/crizotinib in the following.

We first looked at SA- β -gal activity, a well-known senescence marker. While palbociclib and crizotinib alone increased SA- β -gal activity as expected (Fig. 4B and Suppl. Fig. S5B), combined treatment with palbociclib and crizotinib significantly enhanced SA- β -gal activity in the majority of the cell lines. Further, we observed a significantly increased percentage of cells in the G1 or G2/M phase and decreased number of cells in S phase of the cell cycle upon combined compared with mono treatments in all cell lines (Fig. 4C and Suppl. Fig. S5C). However, the reduction in pRb phosphorylation observed after palbociclib treatment was not further enhanced upon combination treatment (Fig. 4D and Suppl. Fig. S5D), possibly since palbociclib directly controls phosphorylation of pRB through inhibition of CDK4/6.

Taken together, these results demonstrate that the combination of palbociclib and crizotinib synergistically enhances the senescence response in melanoma cells.

Treatment with palbociclib and crizotinib modulates the expression of SASP factors and immune-related receptors on melanoma cells

We next monitored the expression of SASP-related genes in the five selected melanoma cell lines upon mono- or combination-treatments with palbociclib and crizotinib. Among the five SASP genes upregulated by palbociclib and/or crizotinib alone, four of them, AREG, IL-1 α , IL-1 β and IL-8, were significantly further increased by combination treatment in A375 cells (Fig.

4E). SASP-related genes induced by mono-treatments in the other 4 cell lines, such as IL-1 α , IL-1 β , IL-8, IL-6, CSF2, were, however, not further enhanced by the combination treatment, except for MMP3 in ESTDAB37 and IL-1 β in ESTDAB140 (Suppl. Fig. S7). This suggests that while the SASP response to palbociclib and crizotinib mono- or combination-treatments among the cell lines was heterogeneous, the most consistent upregulation was observed for IL-1 α , IL-1 β , IL-8 and CSF2.

We next investigated the expression of immune receptors of relevance for natural killer (NK) and T-cell recognition and killing on A375, a long-term established cell line, A375-VR4, it's VEM-resistant variant and KADA, a recently established melanoma cell by FACS. In all three cell lines, palbociclib and to some extent crizotinib increased the expression of HLA class I, but the combination of the two drugs did not lead to further upregulation (Fig. 5A and Suppl. Fig. S8A). Expression of HLA class II was also upregulated in all cell lines by palbociclib, and by crizotinib in KADA (Fig. 5B and Suppl. Fig. S8B). The combination treatment strongly enhanced its expression beyond the mono-treatments only in KADA cells. Finally, PD-L1, which inhibits T and NK cell activation, was increased by palbociclib in all three cell lines and to some extent by crizotinib in KADA. The combined treatment further increased PD-L1 expression only in A375 and A375-VR4 cells, although this did not reach statistical significance in the latter (Fig. 5C and Suppl. Fig. S8C). These results demonstrate that receptors involved in recognition and regulation of T-cells are upregulated on melanoma cells upon palbociclib and crizotinib mono- and combination treatments.

Further, palbociclib upregulated the expression of ULBP 2/5/6, which is a ligand of NKG2D, a receptor involved in NK and T cell activation, in the three cell lines, while crizotinib treatment only increased its expression in KADA (Fig. 5D and Suppl. Fig. S8D). The combination treatment led to further increased expression only in KADA and A375 cells. In KADA cells we also investigated the expression of MIC A/B, another NKG2D ligand, which was induced only by palbociclib, while the combination treatment slightly dampened the upregulation (Suppl. Fig. 8E). Palbociclib and to some extent crizotinib also increased the expression of DR5 and FAS, which both are involved in killing by NK and T cells. However, combined palbociclib and crizotinib treatment did not further increase the expression of these receptors (Suppl. Fig. S8F,

G).

Taken together, this indicates that molecules involved in recognition both by T and NK cells are upregulated by palbociclib and in some cases further increased by combination treatment with crizotinib or staying at the same levels as with palbociclib mono-treatment. On the other hand, the immune checkpoint molecule PD-L1 was also upregulated by palbociclib and further increased by the combination treatment.

Combination treatment with palbociclib and crizotinib inhibits melanoma tumor growth *in vivo* and increases infiltration of CD8+ T-cells and M1 macrophages into tumor tissue.

To address whether senescence induced by palbociclib and crizotinib would affect melanoma tumor growth *in vivo* and to assess any involvement of immune cells in such a response, we next utilized the mouse melanoma cell line YUMM1.7 for syngeneic transplantation into immunocompetent mice. YUMM1.7 is derived from a mouse melanoma tumor carrying BRAF^{V600E} mutation and deletions of PTEN and CDKN2A (34), resembling a subset of human melanomas. First, we studied the senescence response of YUMM1.7 cells *in vitro*. Combination treatment with palbociclib and crizotinib significantly reduced cell growth compared with DMSO and with mono-treatments (Suppl. Fig. 9A). Further, palbociclib and to a lesser extent crizotinib treatment alone led to increased β -gal staining and cell size, indicative of senescence induction, which was further increased by the combination treatment (Suppl. Fig. 9B).

To validate the effect of palbociclib and crizotinib combination treatment on melanoma growth *in vivo*, YUMM1.7 cells were transplanted into the flanks of immunocompetent C57BL/6J mice. Upon palpable tumors, the mice were treated with palbociclib and/or crizotinib or with vehicle for 2 weeks. While single treatments had some effect on tumor growth, the combination treatment significantly inhibited tumor growth and reduced tumor volume (Fig. 6A, B), but none of the treatments had any significant effect on mouse weight (Suppl. Fig. S9C), suggesting lack of serious side effects of the treatments.

We then assessed the effect of the treatments on the immune cell profile in the tumor microenvironment by analyzing different immune cell populations (including T, B, and NK cells, macrophages and neutrophils as well as subtypes of T cells and macrophages) from

dissociated tumors by flow cytometry. The combination treatment had in general a more pronounced effect on immune cell composition than either monotherapy or vehicle (Fig 6C-E). We observed a significant enrichment of T cells and significant reductions of B cells, NK cells and myeloid cells after combination treatment as compared to the mono-treatments and vehicle (Fig. 6C). Among T cells, the combination treatment resulted in a significant increase in CD8⁺ T cells but significant reductions of CD4⁺, $\gamma\delta$ and regulatory T cells (Fig 6D). Looking specifically at macrophages, there was a significant enrichment of M1-like macrophages (CD45⁺, CD11b⁺, F4/80⁺, CD86⁺) after combination treatment compared to mono-treatments, while presence of M2-like macrophages (CD45⁺, CD11b⁺, F4/80⁺, CD204⁺) was unaltered (Fig. 6E).

We next investigated the presence of senescent cells in tumor tissue *in vivo* by β -gal staining (Suppl. Fig. 9D). Few senescent cells were visible in vehicle-treated mice, but there was a substantial increase in β -gal⁺ cells after palbociclib treatment, and some increase after crizotinib treatment, but not to the same extent as after palbociclib treatment. Interestingly, in contrast to treatment of YUMM1.7 cells *in vitro* (Suppl. Fig. 9B), the number of senescent cells decreased after combination treatment compared with palbociclib alone (Suppl. Fig. 9D), suggesting that senescent cells are eliminated after palbociclib + crizotinib-treatment.

To further investigate the influence of CD8⁺ T cells on the tumor-inhibiting effects of the combination treatment, CD8⁺ T cells were removed from the mice by injection of α -CD8 antibodies, and the experiments were repeated. Strikingly, CD8⁺ T cell depletion led to a significant increase in tumor weight compared to control antibodies in palbociclib + crizotinib-treated mice, to a level equivalent to vehicle-treated mice. This suggests that the reduction in tumor weight after combination treatment is at least in part dependent on CD8⁺ T cells (Fig. 6F).

Discussion

Targeted therapies and immunotherapy have revolutionized treatment of metastatic melanoma during recent years. Combined ICI therapy results in long-term survival in up to 50% of patients with advanced melanoma (51). In contrast, targeted therapy eventually

develop resistance leading to tumor relapse, emphasizing the urgent need for new treatment strategies (9,52). Many of the genetic aberrations implicated in drug resistance are known to be involved in senescence regulation, and “pro-senescence therapy” or “therapy-induced senescence (TIS)” have therefore been suggested as an alternative therapeutic approach in such tumors (10-12).

Using a selected number of candidate drugs and compounds in a high throughput fluorescence microscopy-based senescence screen we evaluated the TIS strategy in melanoma. Our results showed that the BRAF^{V600E} inhibitor vemurafenib, the MEK1/2 inhibitor trametinib and the p53-targeting compounds induced senescence in a subset of cell lines. In contrast, the CDK4/6 inhibitor palbociclib, the PI3 kinase inhibitor BKM120 and the MET/ALK/ROS1 inhibitor crizotinib triggered senescence in all or most cell lines, irrespective of *BRAF/NRAS* mutation status. CDK4/6 and PI3K inhibitors have previously been shown to induce senescence in different types of tumor cells, including melanoma cells (53-55), but as far as we know, this is the first report that crizotinib can induce senescence in melanoma cells, and there have been very few reports at all relating senescence-induction to this drug in cancer.

Further, our data show that combination of palbociclib, BKM120 or crizotinib with vemurafenib synergistically enhanced senescence and overcame resistance in *BRAF*^{V600E}-mutant cell lines, which is in line with previous reports regarding palbociclib and PI3K inhibitors (55-57). Our novel finding that vemurafenib and crizotinib combination treatment synergistically induce senescence in vemurafenib-resistant melanoma cells is interesting considering that activation of the HGF/MET-signaling has been suggested as one escape pathway during development of resistance to BRAF- or MEK-inhibitors in BRAF-mutant melanoma (52,58,59).

The most important novel finding from our work is that the combination of palbociclib and crizotinib synergized to further enhance the senescence response in the melanoma cell lines irrespective of *BRAF/NRAS* mutation status. This combination has not been reported in

melanoma therapy so far. Interestingly, upregulation of MET signaling has been implicated in resistance to CDK4/6 inhibition in glioblastoma, and dual inhibition of MET/TRK1 and CDK4/6 could overcome this resistance (60). Senescence induced by palbociclib alone and together with crizotinib was associated with expression of SASP factors such as IL-1 α , IL-1 β , IL-8 and AREG and with increased expression of HLA class I and II (involved in antigen presentation to CD8⁺ and CD4⁺ T-cells, respectively). Palbociclib alone and the combination of palbociclib with crizotinib also increased the expression of PD-L1, which is an immune checkpoint molecule suppressing T-cell and NK cell activation (61,62). This suggests that mono- and combination-treatment with palbociclib and crizotinib induced both positive and negative immune markers with respect to CD8⁺ T cell killing. Moreover, palbociclib and crizotinib and their combination upregulated the expression of the ULBP2/5/6 and MICA/B ligands of the NK cell receptor NKG2D that could both activate NK cells as well as FAS and DR5 death receptors involved in both NK- and T-cell-mediated killing.

Utilizing the syngeneic YUMM1.7 mouse melanoma model, our results showed that palbociclib + crizotinib combination treatment synergistically reduced tumor growth as compared to the mono-treatments. Further, we observed a significant enrichment of CD8⁺ T cells and M1-like macrophages but reductions of CD4⁺ T cells including Treg cells as well as of B cells, NK cells and myeloid cells after combination treatment compared with the mono-treatments and with vehicle. The reduction in NK cells was unexpected considering that these cells have been reported to play an important role in clearance of senescent tumor cells in a KRAS-driven mouse model (53). This indicates that CD8⁺T cells may play a more important role in our model, which is in line with the increased HLA class I expression we observed after treatment. In support of this view, depletion of CD8⁺ T cells resulted in a significant increase in tumor weight, suggesting that the combination treatment of palbociclib and crizotinib indeed enhances CD8⁺ T cell-mediated tumor cell elimination. Interestingly, while the combination treatment increased YUMM1.7 cell senescence in culture, it decreased the number of senescent cells *in vivo* compared with palbociclib alone, indicating increased clearance of senescent cells *in vivo* in response to combination treatment. While senescence induced by palbociclib and other CDK4/6 inhibitors, alone or in combination with other drugs

have been shown to stimulate immune clearance of senescent tumor cells (53,54,63-67), we show here that these effects can be synergistically enhanced by combination treatment with crizotinib in melanoma.

The mechanism behind the synergy between palbociclib and crizotinib with respect to tumor growth inhibition remains to be determined. One possible explanation is that the senescent state becomes more robust and prevents senescence escape pathways more efficiently than single treatments can do. An additional explanation is that the combination treatment reshapes the senescence phenotype in a “senomorphic” way to become more anti-tumorigenic, for instance by modifying the SASP profile or enhancing recognition by the immune cells, thereby affecting their recruitment and activation (10,12,21,25,68-71). It has been reported that treatment with crizotinib in combination with afatinib in melanoma cells downregulates mTOR signaling (38), which is known to affect the composition of SASP (69,70). Furthermore, crizotinib in combination with cisplatin enhanced T cell infiltration and interferon- γ production in a lung cancer model (72), and in another study, MET inhibition blocked recruitment of immunosuppressive neutrophils in a HGF-CDK4^{R24C}-driven mouse melanoma model, thereby improving adoptive T cell transfer or ICI immunotherapy (73). Although MET, rather than ALK or ROS1, is likely the most relevant target of crizotinib in the context of induced senescence in melanoma, this remains to be determined. Clarifying the mechanism(s) by which the combination palbociclib and crizotinib affects the senescence phenotype and immune surveillance in melanoma requires further studies. Another limitation of our study is that it is based on 10 long-term established human melanoma cell lines, and one recently established line. In the future it would be interesting to investigate the effects of combined palbociclib and crizotinib treatment on a broader set of primary melanoma cultures of different types.

In summary, we found that combination of palbociclib and crizotinib induces senescence, SASP and regulation of immune markers in a broad range of human melanoma cells, including BRAF^{V600E}-mutant tumor cells resistant to vemurafenib, NRAS-mutant and non-BRAF/NRAS-mutant melanoma, for which there today are few options for targeted therapy. Importantly, the combination treatment led to a significant reduction of melanoma growth *in vivo*, increase

in CD8+ T cells and M1-type macrophages in the tumor microenvironment, and CD8+ T cell-dependent anti-tumor response to treatment. This suggests that palbociclib/crizotinib-based pro-senescence therapy is potentially an alternative treatment strategy for melanoma. The two drugs are already in clinical use for different indications (74,75), which should facilitate further clinical studies of this combination in patients with melanoma. Considering the increased PD-L1 expression in response to palbociclib and crizotinib treatment, further improvement of treatment could be combining these regimens with ICI, or alternatively senolytic drugs to eliminate senescent tumor cells in a “one-two punch” strategy. These will be interesting options to explore in the future with the aim of improving treatment of patients with malignant melanoma.

Acknowledgements

We thank Dr. Juha Rantala, Misvik Biology, Turku, for advice regarding high-throughput fluorescence microscopy screening. This work was supported by a grant from the Knut and Alice Wallenberg Foundation and by Swedish Cancer Society (Cancerfonden) to LGL.

Author contribution

SEB, JH, RK, GS, KGW, MW, LGL conceptualized and supervised the study, and acquired funding. FZ, LB, ID, JM, MSi, MSt, MA, AA, LD, WB, MDSL, JG, RT, VH, FJ, MW performed experiments, analyzed, visualized and interpreted the data.

FZ, LB, SEB, RK, GS, KGW, MW, LGL wrote the manuscript.

References

1. Schadendorf D, van Akkooi ACJ, Berking C, Griewank KG, Gutzmer R, Hauschild A, *et al.* Melanoma. *Lancet* **2018**;392:971-84
2. Bailey MH, Tokheim C, Porta-Pardo E, Sengupta S, Bertrand D, Weerasinghe A, *et al.* Comprehensive Characterization of Cancer Driver Genes and Mutations. *Cell* **2018**;174:1034-5
3. Hodis E, Watson IR, Kryukov GV, Arold ST, Imielinski M, Theurillat JP, *et al.* A landscape of driver mutations in melanoma. *Cell* **2012**;150:251-63
4. Chapman PB, Hauschild A, Robert C, Haanen JB, Ascierto P, Larkin J, *et al.* Improved survival with vemurafenib in melanoma with BRAF V600E mutation. *N Engl J Med* **2011**;364:2507-16
5. Flaherty KT, Robert C, Hersey P, Nathan P, Garbe C, Milhem M, *et al.* Improved survival with MEK inhibition in BRAF-mutated melanoma. *N Engl J Med* **2012**;367:107-14
6. Robert C, Grob JJ, Stroyakovskiy D, Karaszewska B, Hauschild A, Levchenko E, *et al.* Five-Year Outcomes with Dabrafenib plus Trametinib in Metastatic Melanoma. *N Engl J Med* **2019**;381:626-36
7. Sharma P, Allison JP. Immune checkpoint targeting in cancer therapy: toward combination strategies with curative potential. *Cell* **2015**;161:205-14
8. Wolchok JD, Chiarion-Sileni V, Rutkowski P, Cowey CL, Schadendorf D, Wagstaff J, *et al.* Final, 10-Year Outcomes with Nivolumab plus Ipilimumab in Advanced Melanoma. *N Engl J Med* **2025**;392:11-22
9. Luke JJ, Flaherty KT, Ribas A, Long GV. Targeted agents and immunotherapies: optimizing outcomes in melanoma. *Nat Rev Clin Oncol* **2017**;14:463-82
10. McHugh D, Duran I, Gil J. Senescence as a therapeutic target in cancer and age-related diseases. *Nat Rev Drug Discov* **2025**;24:57-71
11. Nardella C, Clohessy JG, Alimonti A, Pandolfi PP. Pro-senescence therapy for cancer treatment. *Nat Rev Cancer* **2011**;11:503-11
12. Wang L, Lankhorst L, Bernards R. Exploiting senescence for the treatment of cancer. *Nat Rev Cancer* **2022**;22:340-55
13. Lowe SW, Cepero E, Evan G. Intrinsic tumour suppression. *Nature* **2004**;432:307-15
14. Munoz-Espin D, Serrano M. Cellular senescence: from physiology to pathology. *Nat Rev Mol Cell Biol* **2014**;15:482-96
15. Hernandez-Segura A, Nehme J, Demaria M. Hallmarks of Cellular Senescence. *Trends Cell Biol* **2018**;28:436-53
16. Serrano M, Lin AW, McCurrach ME, Beach D, Lowe SW. Oncogenic ras provokes premature cell senescence associated with accumulation of p53 and p16INK4a. *Cell* **1997**;88:593-602
17. Michaloglou C, Vredeveld LC, Soengas MS, Denoyelle C, Kuilman T, van der Horst CM, *et al.* BRAF^{V600E}-associated senescence-like cell cycle arrest of human naevi. *Nature* **2005**;436:720-4
18. Zhuang D, Mannava S, Grachtchouk V, Tang WH, Patil S, Wawrzyniak JA, *et al.* C-MYC overexpression is required for continuous suppression of oncogene-induced

- senescence in melanoma cells. *Oncogene* **2008**;27:6623-34
19. Xue W, Zender L, Miething C, Dickins RA, Hernando E, Krizhanovsky V, *et al.* Senescence and tumour clearance is triggered by p53 restoration in murine liver carcinomas. *Nature* **2007**;445:656-60
 20. Cohn RL, Gasek NS, Kuchel GA, Xu M. The heterogeneity of cellular senescence: insights at the single-cell level. *Trends Cell Biol* **2023**;33:9-17
 21. Faget DV, Ren Q, Stewart SA. Unmasking senescence: context-dependent effects of SASP in cancer. *Nat Rev Cancer* **2019**;19:439-53
 22. Jochems F, Thijssen B, De Conti G, Jansen R, Pogacar Z, Groot K, *et al.* The Cancer SENESCopedia: A delineation of cancer cell senescence. *Cell Rep* **2021**;36:109441
 23. Acosta JC, O'Loghlen A, Banito A, Guijarro MV, Augert A, Raguz S, *et al.* Chemokine signaling via the CXCR2 receptor reinforces senescence. *Cell* **2008**;133:1006-18
 24. Kuilman T, Michaloglou C, Vredeveld LC, Douma S, van Doorn R, Desmet CJ, *et al.* Oncogene-induced senescence relayed by an interleukin-dependent inflammatory network. *Cell* **2008**;133:1019-31
 25. Chibaya L, Snyder J, Ruscetti M. Senescence and the tumor-immune landscape: Implications for cancer immunotherapy. *Semin Cancer Biol* **2022**;86:827-45
 26. Kang TW, Yevsa T, Woller N, Hoenicke L, Wuestefeld T, Dauch D, *et al.* Senescence surveillance of pre-malignant hepatocytes limits liver cancer development. *Nature* **2011**;479:547-51
 27. Campisi J. Aging, cellular senescence, and cancer. *Annu Rev Physiol* **2013**;75:685-705
 28. Pribluda A, Elyada E, Wiener Z, Hamza H, Goldstein RE, Biton M, *et al.* A senescence-inflammatory switch from cancer-inhibitory to cancer-promoting mechanism. *Cancer Cell* **2013**;24:242-56
 29. Hydbring P, Bahram F, Su Y, Tronnorsjo S, Hogstrand K, von der Lehr N, *et al.* Phosphorylation by Cdk2 is required for Myc to repress Ras-induced senescence in cotransformation. *Proc Natl Acad Sci U S A* **2010**;107:58-63
 30. Tabor V, Bocci M, Alikhani N, Kuiper R, Larsson LG. MYC synergizes with activated BRAFV600E in mouse lung tumor development by suppressing senescence. *Cancer Res* **2014**;74:4222-9
 31. Zhu Y, Tchkonja T, Pirtskhalava T, Gower AC, Ding H, Giorgadze N, *et al.* The Achilles' heel of senescent cells: from transcriptome to senolytic drugs. *Aging Cell* **2015**;14:644-58
 32. Ligtenberg MA, Pico de Coana Y, Shmushkovich T, Yoshimoto Y, Truxova I, Yang Y, *et al.* Self-Delivering RNAi Targeting PD-1 Improves Tumor-Specific T Cell Functionality for Adoptive Cell Therapy of Malignant Melanoma. *Mol Ther* **2018**;26:1482-93
 33. Azimi A, Tuominen R, Costa Svedman F, Caramuta S, Pernemalm M, Frostvik Stolt M, *et al.* Silencing FLI or targeting CD13/ANPEP lead to dephosphorylation of EPHA2, a mediator of BRAF inhibitor resistance, and induce growth arrest or apoptosis in melanoma cells. *Cell Death Dis* **2017**;8:e3029
 34. Meeth K, Wang JX, Micevic G, Damsky W, Bosenberg MW. The YUMM lines: a series of congenic mouse melanoma cell lines with defined genetic alterations. *Pigment Cell Melanoma Res* **2016**;29:590-7
 35. Stantic M, Sakil HA, Zirath H, Fang T, Sanz G, Fernandez-Woodbridge A, *et al.* TAp73

- suppresses tumor angiogenesis through repression of proangiogenic cytokines and HIF-1 α activity. *Proc Natl Acad Sci U S A* **2015**;112:220-5
36. Gary RK, Kindell SM. Quantitative assay of senescence-associated beta-galactosidase activity in mammalian cell extracts. *Anal Biochem* **2005**;343:329-34
 37. Zhang F, Bazzar W, Alzrigat M, Larsson LG. Methods to Study Myc-Regulated Cellular Senescence: An Update. *Methods Mol Biol* **2021**;2318:241-54
 38. Das I, Chen H, Maddalo G, Tuominen R, Rebecca VW, Herlyn M, *et al.* Inhibiting insulin and mTOR signaling by afatinib and crizotinib combination fosters broad cytotoxic effects in cutaneous malignant melanoma. *Cell Death Dis* **2020**;11:882
 39. Di Veroli GY, Fornari C, Wang D, Mollard S, Bramhall JL, Richards FM, *et al.* Combenefit: an interactive platform for the analysis and visualization of drug combinations. *Bioinformatics* **2016**;32:2866-8
 40. Monaco G, Chen H, Poidinger M, Chen J, de Magalhaes JP, Larbi A. flowAI: automatic and interactive anomaly discerning tools for flow cytometry data. *Bioinformatics* **2016**;32:2473-80
 41. Maira SM, Pecchi S, Huang A, Burger M, Knapp M, Sterker D, *et al.* Identification and characterization of NVP-BKM120, an orally available pan-class I PI3-kinase inhibitor. *Mol Cancer Ther* **2012**;11:317-28
 42. Toogood PL, Harvey PJ, Repine JT, Sheehan DJ, VanderWel SN, Zhou H, *et al.* Discovery of a potent and selective inhibitor of cyclin-dependent kinase 4/6. *J Med Chem* **2005**;48:2388-406
 43. Shaw AT, Kim DW, Nakagawa K, Seto T, Crino L, Ahn MJ, *et al.* Crizotinib versus chemotherapy in advanced ALK-positive lung cancer. *N Engl J Med* **2013**;368:2385-94
 44. Whittaker SR, Walton MI, Garrett MD, Workman P. The Cyclin-dependent kinase inhibitor CYC202 (R-roscovitine) inhibits retinoblastoma protein phosphorylation, causes loss of Cyclin D1, and activates the mitogen-activated protein kinase pathway. *Cancer Res* **2004**;64:262-72
 45. Middleton MR, Grob JJ, Aaronson N, Fierlbeck G, Tilgen W, Seiter S, *et al.* Randomized phase III study of temozolomide versus dacarbazine in the treatment of patients with advanced metastatic malignant melanoma. *J Clin Oncol* **2000**;18:158-66
 46. Vassilev LT, Vu BT, Graves B, Carvajal D, Podlaski F, Filipovic Z, *et al.* In vivo activation of the p53 pathway by small-molecule antagonists of MDM2. *Science* **2004**;303:844-8
 47. Issaeva N, Bozko P, Enge M, Protopopova M, Verhoef LG, Masucci M, *et al.* Small molecule RITA binds to p53, blocks p53-HDM-2 interaction and activates p53 function in tumors. *Nat Med* **2004**;10:1321-8
 48. Bykov VJ, Issaeva N, Shilov A, Hultcrantz M, Pugacheva E, Chumakov P, *et al.* Restoration of the tumor suppressor function to mutant p53 by a low-molecular-weight compound. *Nat Med* **2002**;8:282-8
 49. Tuval A, Strandgren C, Heldin A, Palomar-Siles M, Wiman KG. Pharmacological reactivation of p53 in the era of precision anticancer medicine. *Nat Rev Clin Oncol* **2024**;21:106-20
 50. Smyth LM, Monson KR, Jhaveri K, Drilon A, Li BT, Abida W, *et al.* A phase 1b dose expansion study of the pan-class I PI3K inhibitor buparlisib (BKM120) plus carboplatin and paclitaxel in PTEN deficient tumors and with dose intensified carboplatin and

- paclitaxel. *Invest New Drugs* **2017**;35:742-50
51. Weiss SA, Kluger H. CheckMate-067: Raising the Bar for the Next Decade in Oncology. *J Clin Oncol* **2022**;40:111-3
 52. Hugo W, Shi H, Sun L, Piva M, Song C, Kong X, *et al.* Non-genomic and Immune Evolution of Melanoma Acquiring MAPKi Resistance. *Cell* **2015**;162:1271-85
 53. Ruscetti M, Leibold J, Bott MJ, Fennell M, Kulick A, Salgado NR, *et al.* NK cell-mediated cytotoxicity contributes to tumor control by a cytostatic drug combination. *Science* **2018**;362:1416-22
 54. Vilgelm AE, Johnson CA, Prasad N, Yang J, Chen SC, Ayers GD, *et al.* Connecting the Dots: Therapy-Induced Senescence and a Tumor-Suppressive Immune Microenvironment. *J Natl Cancer Inst* **2016**;108:djv406
 55. Vredeveld LC, Possik PA, Smit MA, Meissl K, Michaloglou C, Horlings HM, *et al.* Abrogation of BRAFV600E-induced senescence by PI3K pathway activation contributes to melanomagenesis. *Genes Dev* **2012**;26:1055-69
 56. Deuker MM, Marsh Durban V, Phillips WA, McMahon M. PI3¹-kinase inhibition forestalls the onset of MEK1/2 inhibitor resistance in BRAF-mutated melanoma. *Cancer Discov* **2015**;5:143-53
 57. Yoshida A, Lee EK, Diehl JA. Induction of Therapeutic Senescence in Vemurafenib-Resistant Melanoma by Extended Inhibition of CDK4/6. *Cancer Res* **2016**;76:2990-3002
 58. Cheng H, Chua V, Liao C, Purwin TJ, Terai M, Kageyama K, *et al.* Co-targeting HGF/cMET Signaling with MEK Inhibitors in Metastatic Uveal Melanoma. *Mol Cancer Ther* **2017**;16:516-28
 59. Straussman R, Morikawa T, Shee K, Barzily-Rokni M, Qian ZR, Du J, *et al.* Tumour micro-environment elicits innate resistance to RAF inhibitors through HGF secretion. *Nature* **2012**;487:500-4
 60. Olmez I, Zhang Y, Manigat L, Benamar M, Brenneman B, Nakano I, *et al.* Combined c-Met/Trk Inhibition Overcomes Resistance to CDK4/6 Inhibitors in Glioblastoma. *Cancer Res* **2018**;78:4360-9
 61. Iwai Y, Ishida M, Tanaka Y, Okazaki T, Honjo T, Minato N. Involvement of PD-L1 on tumor cells in the escape from host immune system and tumor immunotherapy by PD-L1 blockade. *Proc Natl Acad Sci U S A* **2002**;99:12293-7
 62. Qiao DR, Cheng JY, Yan WQ, Li HJ. PD-L1/PD-1 blockade enhanced the cytotoxicity of natural killer cell on the non-small cell lung cancer (NSCLC) by granzyme B secretion. *Clin Transl Oncol* **2023**;25:2373-83
 63. Deng J, Wang ES, Jenkins RW, Li S, Dries R, Yates K, *et al.* CDK4/6 Inhibition Augments Antitumor Immunity by Enhancing T-cell Activation. *Cancer Discov* **2018**;8:216-33
 64. Goel S, DeCristo MJ, Watt AC, BrinJones H, Sceneay J, Li BB, *et al.* CDK4/6 inhibition triggers anti-tumour immunity. *Nature* **2017**;548:471-5
 65. Jerby-Arnon L, Shah P, Cuoco MS, Rodman C, Su MJ, Melms JC, *et al.* A Cancer Cell Program Promotes T Cell Exclusion and Resistance to Checkpoint Blockade. *Cell* **2018**;175:984-97 e24
 66. Lelliott EJ, Kong IY, Zethoven M, Ramsbottom KM, Martelotto LG, Meyran D, *et al.* CDK4/6 Inhibition Promotes Antitumor Immunity through the Induction of T-cell Memory. *Cancer Discov* **2021**;11:2582-601

67. Ruscetti M, Morris JPt, Mezzadra R, Russell J, Leibold J, Romesser PB, *et al.* Senescence-Induced Vascular Remodeling Creates Therapeutic Vulnerabilities in Pancreas Cancer. *Cell* **2020**;181:424-41 e21
68. Chen HA, Ho YJ, Mezzadra R, Adrover JM, Smolkin R, Zhu C, *et al.* Senescence Rewires Microenvironment Sensing to Facilitate Antitumor Immunity. *Cancer Discov* **2023**;13:432-53
69. Herranz N, Gallage S, Mellone M, Wuestefeld T, Klotz S, Hanley CJ, *et al.* mTOR regulates MAPKAPK2 translation to control the senescence-associated secretory phenotype. *Nat Cell Biol* **2015**;17:1205-17
70. Laberge RM, Sun Y, Orjalo AV, Patil CK, Freund A, Zhou L, *et al.* MTOR regulates the pro-tumorigenic senescence-associated secretory phenotype by promoting IL1A translation. *Nat Cell Biol* **2015**;17:1049-61
71. Marin I, Boix O, Garcia-Garijo A, Sirois I, Caballe A, Zarzuela E, *et al.* Cellular Senescence Is Immunogenic and Promotes Antitumor Immunity. *Cancer Discov* **2023**;13:410-31
72. Liu P, Zhao L, Kepp O, Kroemer G. Crizotinib - a tyrosine kinase inhibitor that stimulates immunogenic cell death. *Oncoimmunology* **2019**;8:1596652
73. Glodde N, Bald T, van den Boorn-Konijnenberg D, Nakamura K, O'Donnell JS, Szczepanski S, *et al.* Reactive Neutrophil Responses Dependent on the Receptor Tyrosine Kinase c-MET Limit Cancer Immunotherapy. *Immunity* **2017**;47:789-802 e9
74. Louveau B, Resche-Rigon M, Lesimple T, Da Meda L, Pracht M, Baroudjian B, *et al.* Phase I-II Open-Label Multicenter Study of Palbociclib + Vemurafenib in BRAF (V600MUT) Metastatic Melanoma Patients: Uncovering CHEK2 as a Major Response Mechanism. *Clin Cancer Res* **2021**;27:3876-83
75. Spring LM, Wander SA, Andre F, Moy B, Turner NC, Bardia A. Cyclin-dependent kinase 4 and 6 inhibitors for hormone receptor-positive breast cancer: past, present, and future. *Lancet* **2020**;395:817-27

Table 1. Melanoma cell lines and drugs used in the senescence screen

Melanoma cell lines

Cell lines	Genetic alterations
A375	BRAF p.V600E, CDKN2A p.E61.*; E69*
ESTDAB-049 (Mel-624)	BRAF p.V600E, TP53 p.C275W
SKMEL-28	BRAF p.V600E, CDK4 p.R24C, PTEN T167A, TP53 p.L145R
ESTDAB-037 (IGR-39)	BRAF p.V600E, ΔPTEN, MYC gain
ESTDAB-102 (Ma-Mel-28)	NRAS p.Q61R,
ESTDAB-149 (Ma-Mel-105)	NRAS p.Q61R, PTEN p.K128N, ΔCDKN2A
SKMEL-2	NRAS p.Q61R, PIK3C3 p.R768W, TP53 p.G245S
ESTDAB-140 (Ma-Mel-42a)	CDK4 gain, PIK3CA p.N345K
ESTDAB-138 (Ma-Mel-15)	Cyclin D1 gain
ESTDAB-105 (Ma-Mel-8a)	Δp16 ^{INK4A} , Δp14 ^{ARF} , PTEN p. E157* and D162V, TP53 p.R283C
KADA	TP53 p.K248W, NF1 p.Q531*

Drugs

Drug	Abb.	Target	MOA
Vemurafenib	VEM	BRAFV600E	Inhibitor of the BRAFV600E mutated kinase
Trametinib	TRA	MEKi	Inhibits MEK1/2 kinases
Temozolomide	TMZ	DNA alkylator	Alkylates/methylates DNA
BKM120	BKM	PI3K	Inhibitor of PI3 kinases p110a/b/d/g
Crizotinib	CRIZ	ALK, MET, ROS1	Inhibitor of ALK/MET/ROS1 kinases
Palbociclib	PAL	CDK4/6	Inhibitor of CDK4/6 kinases
Selaciclib	SEL	CDK2/CDK1	Inhibitor of CDK2/CDK1 kinases
Nutlin	NUT	MDM2/p53	Stabilizes p53 by blocking p53:MDM2 interaction
APR-246	APR	p53/Redox	Reactivates mutant p53/perturbs redox homeostasis
RITA	RITA	p53	Inhibits MDM2:p53 interaction

Upper panel: melanoma cell lines in the screen with corresponding genetic alterations.

Lower panel: List of ten selected targeted agents used in the screen, their abbreviations in the figures and their mechanism of action (MOA).

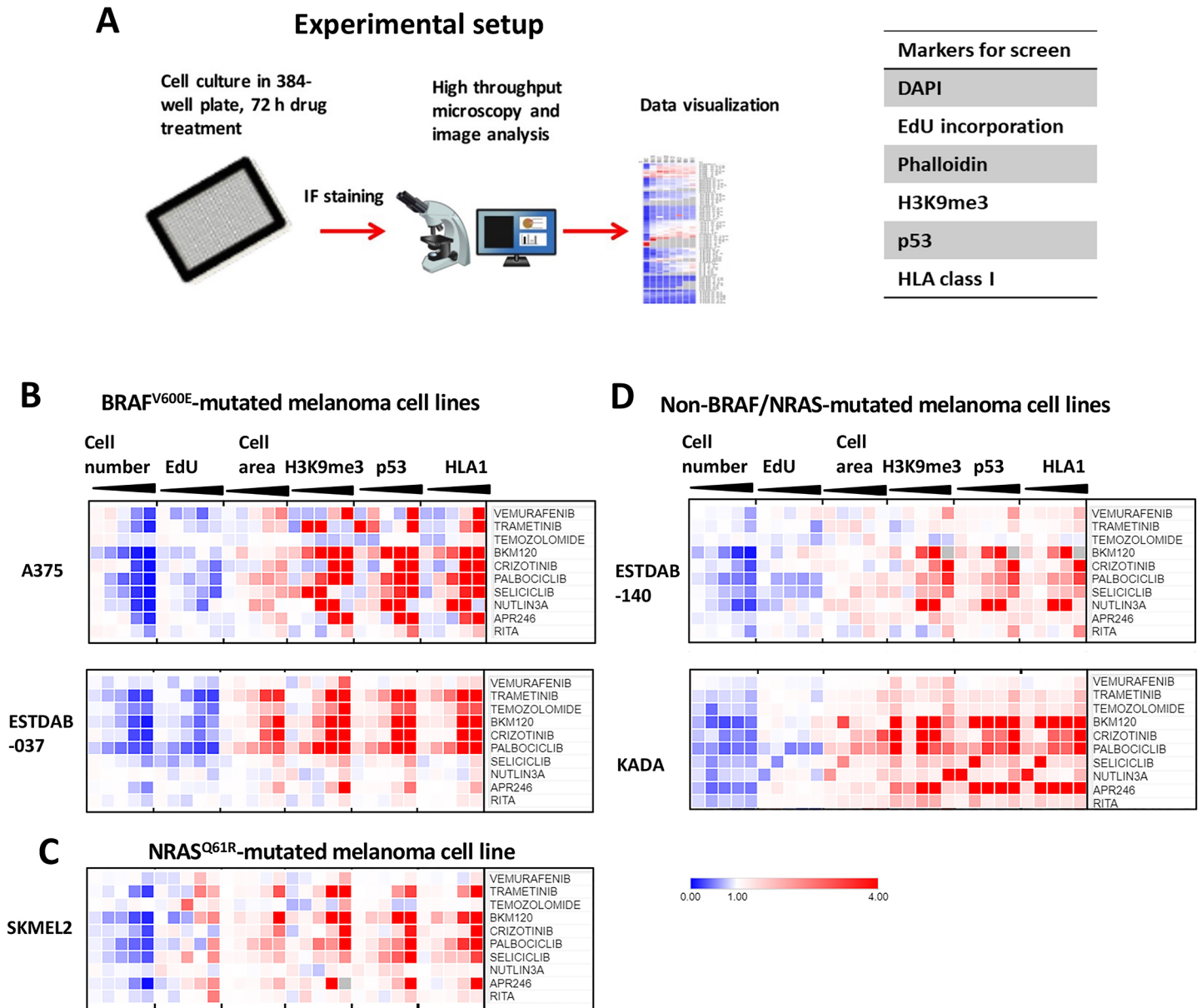
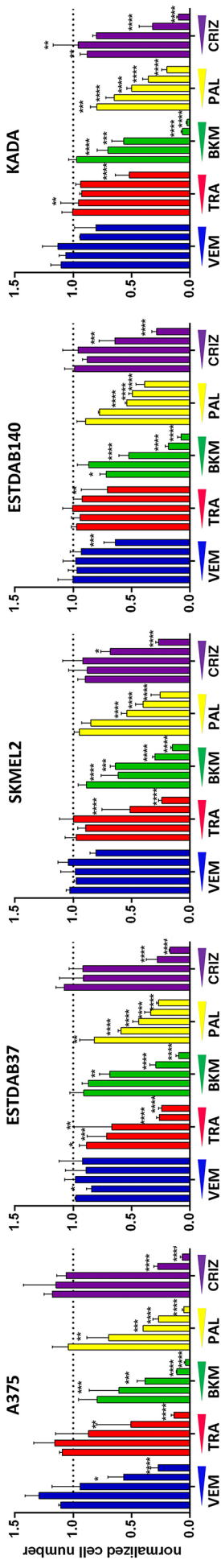


Figure 1

Figure 1. Screen for drug-induced senescence in human melanoma cell lines (A) Experimental set-up and workflow of the drug-induced senescence screen. Right panel: Markers used in the screen, DAPI (cell number), EdU incorporation, phalloidin (cell area), H3K9me3, p53 and HLA class I immunofluorescence staining. (B-D) Heatmaps showing data from measurements of the six biomarkers in response to 11 selected drugs after 72 hours of treatment in 5 selected melanoma cell lines. Drug concentrations are specified in Supplementary Table 1A and increasing concentration are illustrated as wedges. (B) A375 and ESTDAB037, both with BRAF^{V600E} mutation; (C) SKMEL2 with NRAS^{Q61R} mutation; (D) ESTDAB140 and KADA, with non-BRAF/NRAS mutations. Intensity per field was normalized to DMSO and median values (%) were presented here with indicated color code.

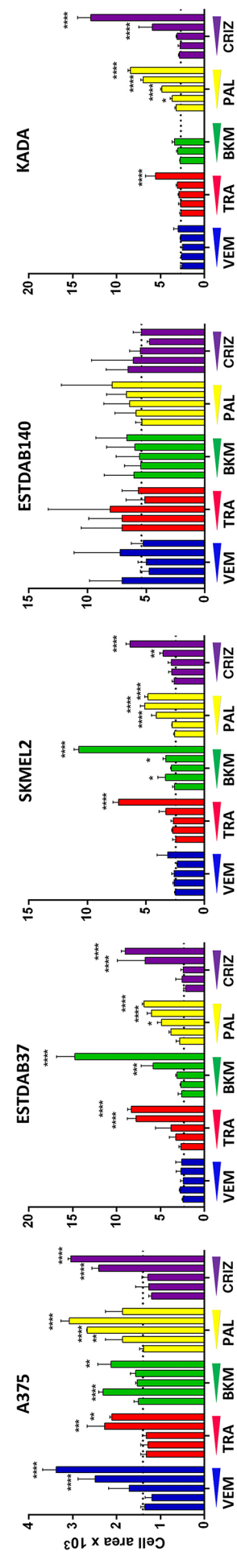
A

Cell number



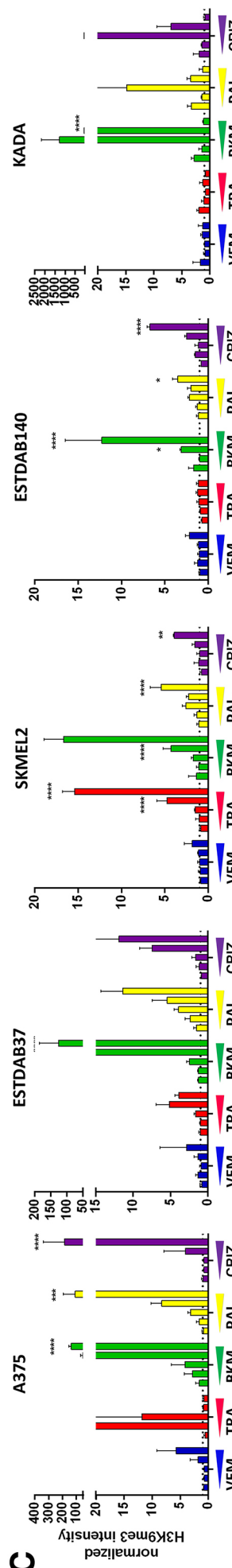
B

Cell size



C

Heterochromatin foci



D

HLA class I expression

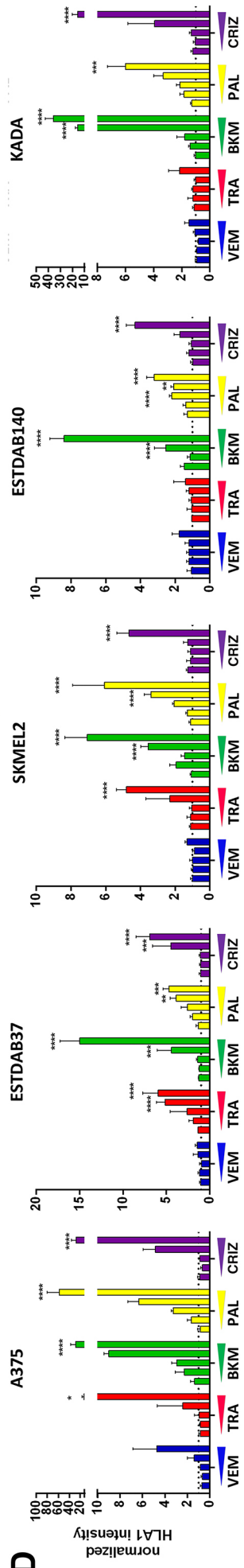


Figure 2. Validation of senescence induction in response to selected drugs in selected melanoma cell lines. Single-drug treatment of A375, ESTDAB37, SKMEL2, ESTDAB140 and KADA with vemurafenib (VEM), trametinib (TRA), BKM120 (BKM), palbociclib (PAL) or crizotinib (CRIZ) for 3 days. Bar charts illustrating cell number (A), cell size (B), intensity of H3K9me3 (C) and HLA class I (D) stainings. Drug concentrations are specified in Supplementary Table 1A and increasing concentration are illustrated as wedges. Data was normalized to DMSO treatment and mean±SEM values are presented. The value for DMSO for each marker is indicated as a dotted line in the figure. Blue: VEM; red: TRA; green: BKM; yellow: PAL; purple, CRIZ. * p< 0.05; ** p< 0.01, *** p<0.001, **** p<0.0001.

Figure 3. Drug combination senescence screen using vemurafenib-sensitive and vemurafenib-resistant melanoma cell lines. Combination treatment using vemurafenib (VEM) together with temozolomide (TMZ), BKM120 (BKM), crizotinib (CRIZ) or palbociclib (PAL) at 2-fold serial dilutions for 72 hours in A) A375, B) A375-VR4 and C) ESTDAB37 cells. The highest concentrations of the drugs in each combination are listed in Suppl. Table 2A and increasing concentrations for each drug are illustrated as black wedges. D=DMSO. The heatmaps show data representing cell number, percentage of EdU positive cells, cell size and combination synergy index based on cell size in A375, A375-VR4 (acquired VEM-resistance) and ESTDAB37 (intrinsic VEM-resistance) cells. Cell number and cell size were normalized to DMSO-treated cells. Missing data due to too low cell number as a result of cell death is indicated as grey. Green = synergism, yellow = antagonism.

Combination treatment palbociclib with crizotinib

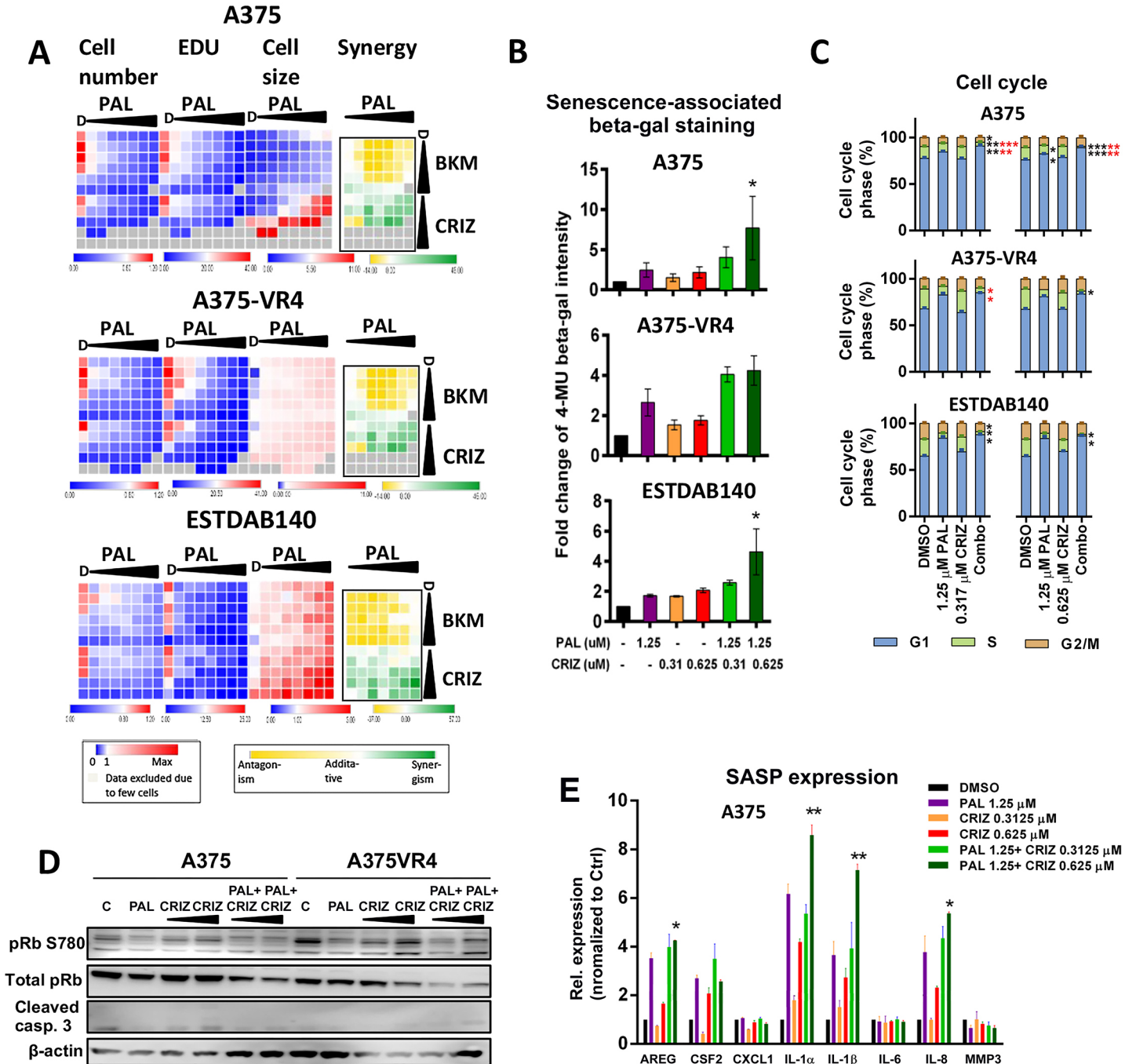


Figure 4

Figure 4. Drug combination senescence screen using selected melanoma cell lines. (A) Combination treatment using PAL together with BKM or CRIZ at 2-fold serial dilutions for 72 hours. The highest doses of the drugs are listed in Suppl. Table 2B. The heatmaps show data representing cell number, percentage of EdU positive cells, cell size and combination synergy index based on cell size in A375, A375-VR4 and ESTDAB140 cells. Missing data due to too low cell number as a result of cell death is indicated as grey. Green = synergism, yellow = antagonism. (B) Fluorescent β -galactosidase assay (MUG) after mono or combination treatment with PAL and CRIZ as indicated. (C) Cell cycle analysis after mono or combination treatment with PAL and CRIZ in indicated cell lines for 72 hours. (D) Western blot analysis of S780 phosphorylated pRB, total pRB and cleaved caspase 3 after mono or combination treatment with a fixed concentration of PAL (1.25 μ M) and increasing concentrations of CRIZ (0.31 and 0.63 μ M as illustrated by wedges) in the indicated cell lines for 72 hours. (E) Relative fold change of SASP-related gene expression in A375 cells in response to combination treatment using palbociclib (PAL) and crizotinib (CRIZ) for 72 hours. Biological triplicates were presented as mean \pm SEM and one-way ANOVA was applied to compare drug treatment versus mono-therapy, * $p < 0.05$; ** $p < 0.01$, * $p < 0.05$; ** $p < 0.01$, *** $p < 0.001$. Black stars represent significance DMSO control vs. treatments, red stars represent significance CRIZ vs. combination treatment.

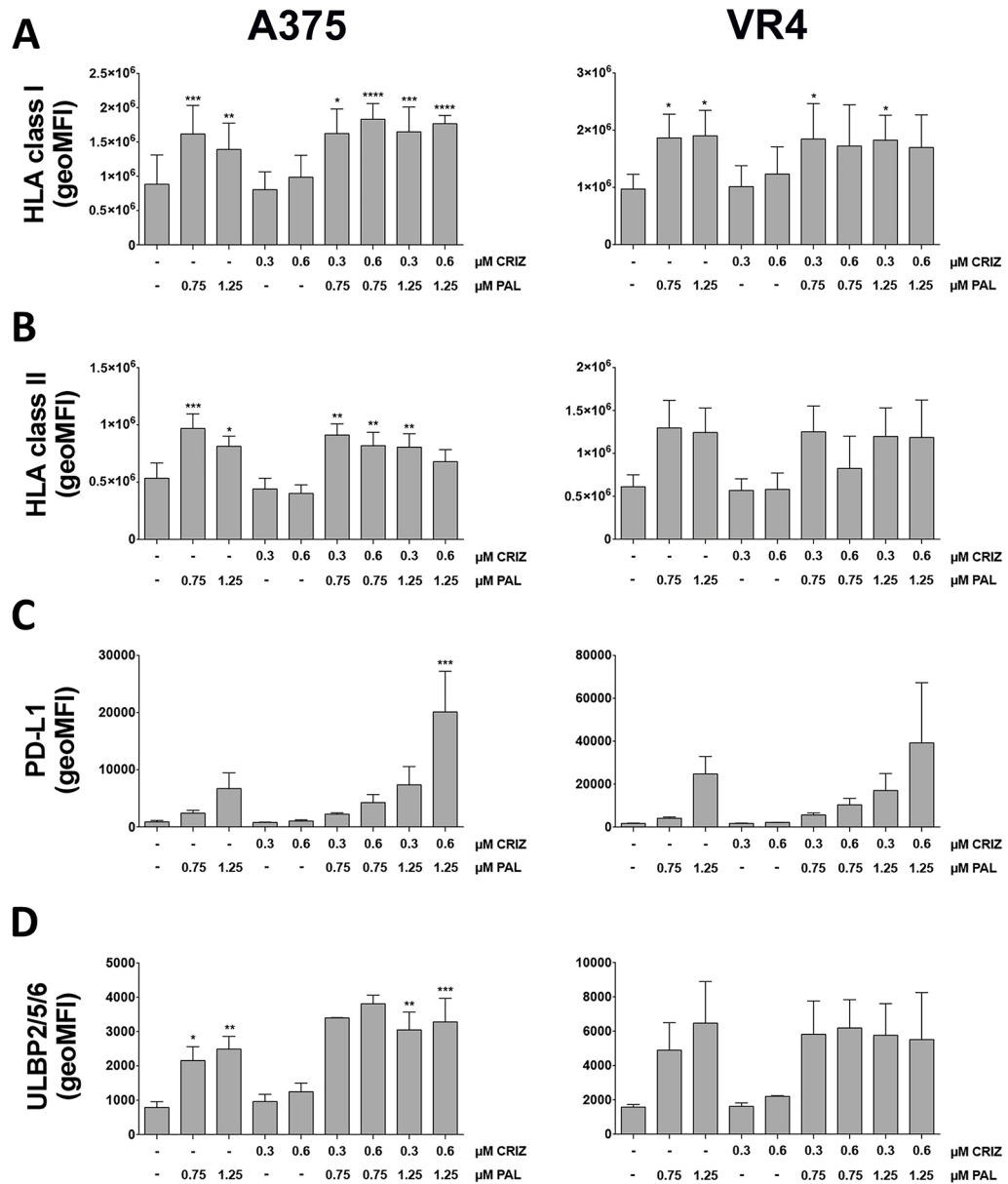
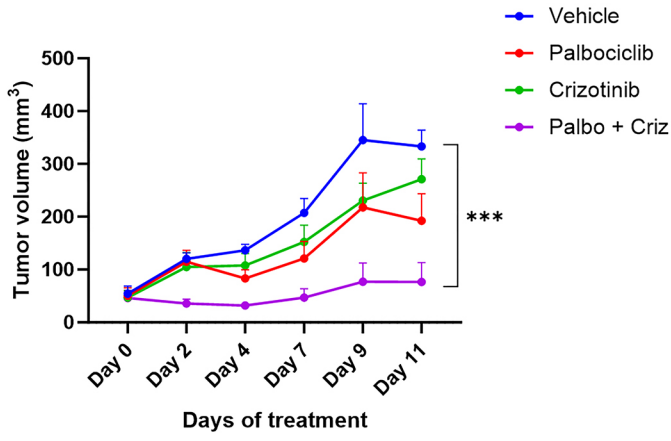


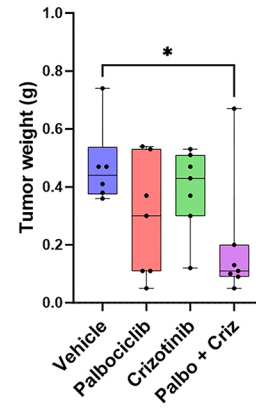
Figure 5

Figure 5. Expression of immune markers regulating recognition by T cells and NK cells upon combination treatment with palbociclib and crizotinib. A375 (left panel) and A375-VR4 (right panel) cells were treated with indicated concentrations of PAL and/or CRIZ for 72 hrs followed by analysis of (A) HLA class I, (B) HLA class II, (C) PD-L1 and (D) ULBP2/5/6 by flow cytometry using specific antibodies.

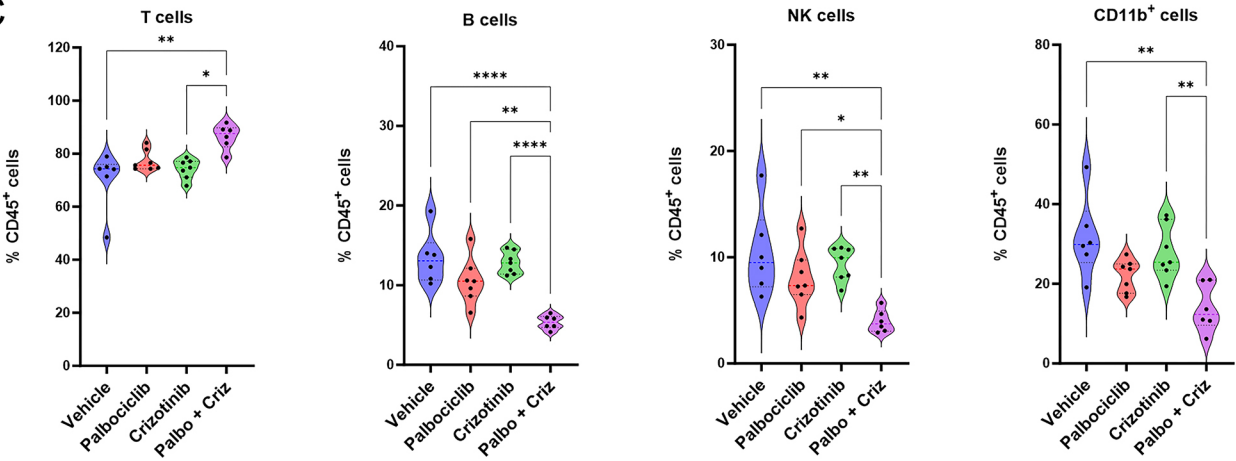
A



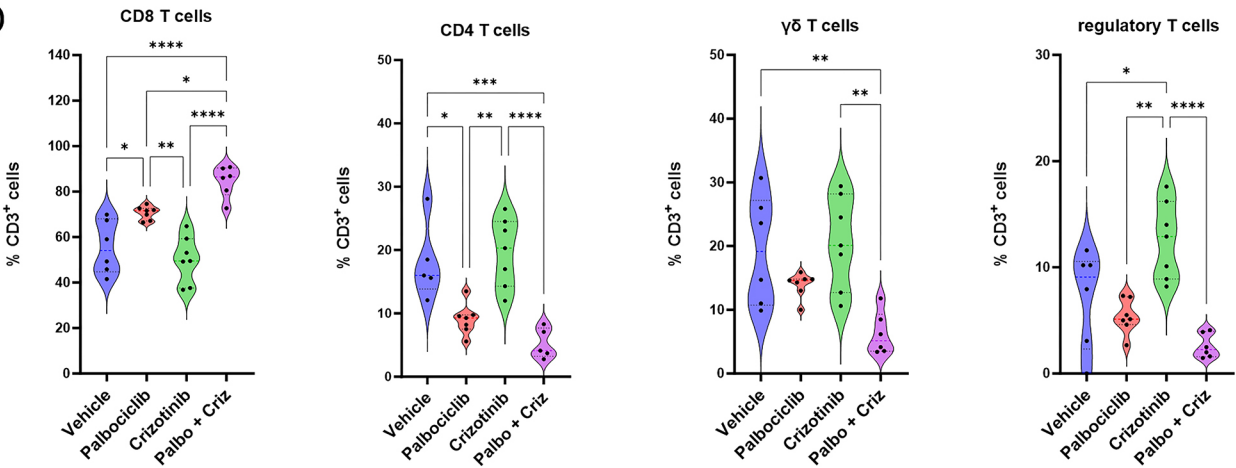
B



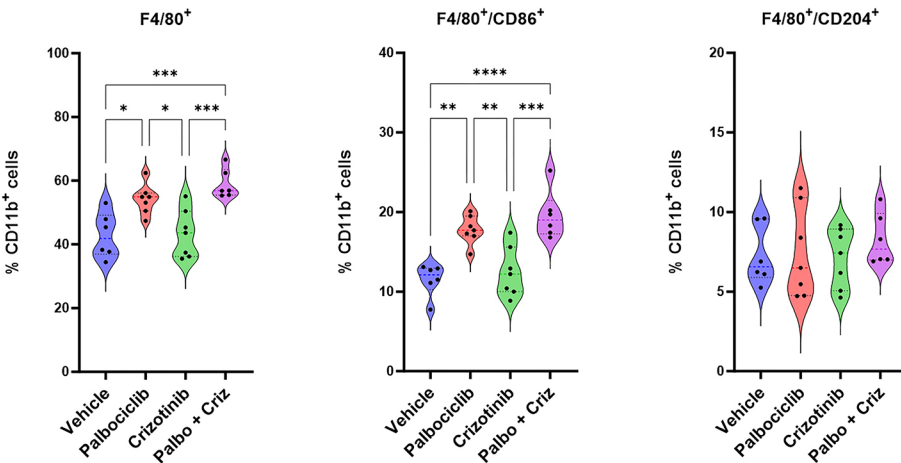
C



D



E



F

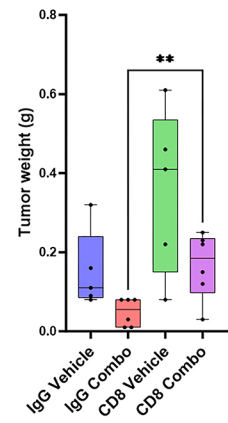


Figure 6

Figure 6. Effects of combination treatment using palbociclib (Palbo) and crizotinib (Criz) on tumor growth and immune cell infiltration after syngeneic transplantation of YUMM1.7 melanoma cells into immunocompetent C57BL6 mice. (A) YUMM1.7 tumor volume measurement during treatment period (11 days), data shown are Mean \pm SEM (B) Violin box showing YUMM1.7 tumor weight measurement at endpoint (C-E) Violin box showing frequencies of infiltrating immune cells as determined by flow cytometry. (C) Analysis of total T, B, NK and myeloid cells. (D) Analysis of subpopulations of T cells as indicated (D) Analysis of total, M1-like and M2-like macrophages. Differences between vehicle and treatment conditions were assessed by one-way ANOVA test, * $p < 0.05$; ** $p < 0.01$; *** $p < 0.001$, **** $p < 0.0001$ - Represented points for (A), (B) and (C-E): Vehicle, $n=6$; Palbo, $n=7$; Criz, $n=7$; Palbo + Criz, $n=7$. (F) Effects of CD8+ T cell depletion on tumor growth. Anti-mouse CD8a or IgG2b isotype control antibodies were injected i.p. into tumor-bearing mice two days before the start of drug treatment, followed by administration every 4 days during the course of the experiment. Difference between IgG Combo and CD8 Combo was assessed by unpaired t-test, ** $p = 0.0096$. Represented points for (F): -IgG Vehicle, $n=5$; IgG Combo, $n=6$; CD8 Vehicle, $n=5$; CD8 Combo, $n=6$.